A new ultrasonic method for measuring elastic moduli in unsupported thin films: Application to Cu-Pd superlattices.

A. Moreau and J. B. Ketterson,

Department of Physics and Astronomy,

B. Davis,

Materials Science and Engineering Department,

Northwestern University,

Evanston, IL 60208

Abstract

We have developed a new ultrasonic method for measuring the phase velocity of longitudinal and shear waves in self-supporting thin films. The film is bonded at one end to an interdigital transducer (IDT) which emits a continuous wave signal. The film is supported at the other end and maintained flat under a weak tension. A receiving IDT detects the in-phase and quadrature components of the sound waves as they propagate. A liquid bond is used between the receiving IDT and the film to allow a continuous variation of the path length. From the longitudinal and shear wave velocities, we can deduce the flexural and shear moduli of the film. For films of uniaxial or higher symmetry, the Young's and biaxial moduli can be expressed as combinations of the flexural and shear moduli. We applied this technique to Cu-Pd composition modulated thin films. Contrary to previous reports, we have not observed the supermodulus effect in either the flexural, shear, Young's or biaxial moduli for modulation wavelengths between 13 and 36 Å.

1 Introduction

Relatively few techniques exist to measure the ultrasonic velocity in self-supporting thin films. One of the oldest is the measurement of the propagation delay time of an rf pulse, using either a transmission technique, involving an emitting and a receiving transducer located at each end of the film,[1] or using a single transducer in a pulse-echo configuration.[2,3] Recently, mechanical transducers have been replaced by pulsed laser excitation and laser interferometric detection.[4,5,6] It is also possible to use surface sensitive techniques such as ultrasonic detection using the angular deviation of a reflected laser beam, surface grating abd reflectivity techniques, and Brillouin scattering. To our knowledge, only Brillouin scattering has been used on self-supporting thin films.[7]

In this paper, we first present a new method which relies on the measurement of the real and imaginary components of the amplitude of a continuous ultrasonic wave as a function of position. This method is adequate for measuring the Lamb symmetric (S0) and the horizontal shear (SH) vibration modes from which the flexural (F) and the normal shear (S_z) elastic moduli can be calculated. Its main advantages over other methods are its simplicity and low cost, while maintaining comparable accuracy ($\leq 1\%$ at 10 MHz for a path length (l) of 5 mm, and improving linearly with l). We then compare measurements on films of pure metals with a good [111] texture, to the expected values calculated from bulk elastic constants. Finally, we measure the change in the elastic moduli of Cu-Pd composition modulated multilayers as a function of the modulation wavelength.

2 Experimental Set-up

2.1 Transducers

Our method employs two interdigital transducers (IDT's), one as an emitter and one as a receiver. Each transducer has 27 Cu electrodes (0.1 mm wide, 3.8 mm long, 0.5 micron thick and separated by 0.1 mm) which were patterned by photolithography onto a lithium niobate piezoelectric substrate. For completeness, we describe the action of the transducers. When an AC potential is applied to alternate electrodes (see Fig. 1), the resulting electric field sets the surface of the IDT into motion. If the wavelength of the surface waves is equal to twice the spacing between the electrodes, then the contribution from each pair of fingers adds coherently. For our transducers, this resonant frequency was 10.3 MHz. Conversely, when the piezoelectric substrate vibrates, it induces an electric potential which is detected by the electrodes and the IDT behaves as a receiver.

Depending on the orientation of the lithium niobate crystal surface and on the direction of propagation of the generated Rayleigh waves, the motion can have displacement components in either 2 or 3 dimensions:[8] longitudinal and shear vertical (i.e., normal to the surface) components are always present, while shear horizontal components are absent for only a few geometries. When all three components are present, it is possible to generate all three vibration modes of thin films; these are the Lamb symmetric (S0) or pressure wave, the Lamb antisymmetric (A0) or flexural wave and the horizontal shear (SH) wave. If the horizontal shear displacement component of the substrate is absent, the SH wave will be suppressed.

2.2 Thin Film

Great care must be exercised in handling the films. The thinnest ones (on the order of 1 micron thick) are detached from their mica substrate by dipping them at a shallow angle in water. The surface tension combined with the infiltration of water between the substrate and the film help them separate. Sometimes a razor blade is used to gently lift off a corner. Other tricks such as deposition on a different substrate or predeposition of a soluble layer may be used.

Once the film has been removed, it is rinsed in alcohol and dried in air. Then it is cut into a rectangular strip using a sharp razor blade. It is important to cut the film as neatly as possible to avoid spurious sound reflection or diffraction from jagged edges and kinks. The 2 mm width of the strip insures that the film is much narrower than the electrode's length. This allows us to use only the center part of the emitting IDT's active area and avoid the diffraction associated with the edges. To mount the film onto the edge of the emitting IDT (see Fig. 1) we proceed as follows: first, all but the edge of the film to be bonded onto the surface of the IDT is covered. The exposed part of the film is then sprayed with 3M Photomount Spray Adhesive (Adhesives, Coatings and Sealers Division/3M, St. Paul, MN 55144) and gently pressed to the surface of the emitting IDT. A small weight is used to apply a uniform pressure across the bond while it settles. This method was chosen since it yields a relatively flat and uniform bond, which is essential if the the plane waves traveling on the surface of the IDT are to be transmitted as plane waves in the film. For less delicate thin foils (commercial aluminum foil for example), most bonds that are sufficiently uniform will transmit enough ultrasonic energy.

The other end of the film is varnished onto a small (4x4 mm) piece of mica. One

end of a fine string (fine dental floss) is also varnished to the mica (Fig. 1). By applying a week force (of the order of 10^{-3} N) to the opposite end of the string, the film is pulled to a horizontal position.

2.3 Liquid bond

As mentioned in the introduction, the experiment consists of sending a continuous wave into the film and of detecting its in-phase and quadrature amplitudes as it propagates. To do so, we position the receiving IDT vertically above the film (Fig. 1) and we slide the emitting IDT/film assembly underneath. The ultrasonic continuity between the film and the receiving IDT is provided by a liquid bond. We use a drop of castor oil because of its viscoelastic properties and its low vapor pressure. It can also be easily removed from the film and the transducer using a cotton swab and ethanol. Due to the oil surface tension, the film tends to "stick" to the receiving IDT and makes the bond very thin. We find that the ultrasonic absorption in the bond, although not negligible, does not present a problem.

The size of the drop determines the position resolution of the experiment: sound waves with wavelengths less than the size of the bond ($\approx$ 1.0 mm) are expected to be averaged out. In practice, the maximum achievable resolution (about 0.15 mm) is much better, possibly because a small portion of the bond transmits most of the signal. For a signal frequency of 10.3 MHz, this means that we will not be able to observe the slow moving flexural waves which have a wavelength of about 35 microns (for our typically 1.5 μm thick films).

Due to the surface tension of castor oil and the slow scanning speed used, most

of the oil stays on the receiving transducer. However, there inevitably remains a trace and for this reason we only sweep the receiver in the direction towards the emitter. Moreover, kinks, dirt particles and imperfections in the film can affect the local shape of the bond, resulting in effective positional errors and in total amplitude errors. This is believed to be the major source of error in this experiment. However, as the path length increases, the positional errors average out and the accuracy of the measurement improves. The amplitude error is not a large factor in measuring the wave vector, k, which is more sensitive to the phase than to the amplitude of the signal. On the other hand, this technique is not adequate for the measurement of absorption coefficients.

2.4 Apparatus

The apparatus used is shown schematically in Fig. 2. It has two major components: the receiving IDT holder, which is fixed (left of Fig. 2a), and the sample holder, which is mounted on a horizontal translation stage (right of Fig. 2a and Fig. 2b).

The receiving IDT's holder allows vertical positioning of the IDT enclosure (a) through the vertical translator (b) as well as "pitch" and "yaw" angular positioning of the IDT enclosure using an optical mount (c). The "pitch" angle is set to 90° so that the receiving IDT (d) is perpendicular to the film. The "yaw" angle is used to align the receiving IDT so that it is parallel to the ultrasonic wavefront. The receiving IDT enclosure (a) is made of brass to shield out the electromagnetic radiation produced by the emitting IDT (e). The electrical detected by the transducer is directed by a twisted pair of wires to a miniature coaxial connector (not shown) located at the top of the enclosure. In this way, only the bottom edge of the IDT, which does not have any electrodes, is exposed to the radiation.

The sample holder assembly is mounted on a brass plate (f) which is screwed onto an Oriel precision translator (g) and can be removed so that the sample holder can be used in other experiments.[9] The translator is driven by a DC motor (h) which has an optical shaft encoder and a position resolution of ±0.3 microns. The motor can be operated either manually or through a computer interface.

The emitting IDT (e) is glued to the surface of a brass block (i). A brass plate (j) covers it to limit the amount of electromagnetic radiation emitted. Again, the electrical signal is brought to a miniature coaxial cable connector situated next to the IDT (not shown). The translator (k) to the right of the block controls the amount of tension in the string (l) and in the film (m). The string can be either attached to the translator, or held in place with a weight (n).

It is also important to ground the metallic thin film to be measured. If it is not grounded, the film will behave as an antenna. Shielding is more important in a continuous wave than in a pulsed experiment because the electromagnetic feedthrough is superimposed on the ultrasonic signal and may contribute a significant background signal. However, no precaution other than a good design was required.

2.5 Electronics

The electronics set-up is shown in Fig. 3. A 300 mV, 10.3 MHz continuous wave is produced by the rf generator, amplified to approximately 7 V and fed to the emitting IDT. It is also sent to a 90° power divider, the outputs of which provide two reference rf signals that differ by a constant phase of 90°. The waveform generated by the receiving IDT is amplified and mixed with the two reference signals. Since the

reference and detected signals are at the same frequency, the output of each mixer consists of 20.6 MHz and DC components. The 20.6 MHz component is filtered out and the magnitude of the DC component is proportional to the projection of the detected signal onto the reference signal. Thus the two DC outputs can be viewed as the real and imaginary components (to an arbitrary phase constant and amplitude scale) of the ultrasonic complex amplitude.

In order to use sensitive lock-in detection, we switch the rf generator on and off at a low frequency (94 Hz). The detected outputs then alternate between zero and the steady state values and are applied to the lock-in's inputs. The analog outputs of the lock-in amplifiers are digitized and read by a computer. The computer also controls and monitors the precision translator's motion via a DC motor driver/controller.

The integration time constants of the lock-in's were set to 1 s. A typical scan consists of 256 data points, separated by 20 μm with the sweep rate set to 1 μm/s and with a 5 second pause to let the lock-in outputs settle before they are read. The real component of one such scan is shown as dots in Fig. 4.

3 Data analysis

We first perform a complex discrete Fourier transform on the recorded complex amplitudes. By squaring the amplitudes as a function of k, we obtain a power spectrum where each peak represents an excited vibration mode (see Fig. 5). Up to 4 peaks can be observed: longitudinal and shear modes together with their reflections. However, the reflected signals can be artificially introduced or removed if the signal gain is not identical for the two real and imaginary channels. On the other hand, if these gains are known, the data can be numerically adjusted later on.

Due to the discrete nature of the calculation, the accuracy, Δk, in the measurement of the wave vector, k, is limited to $\Delta k = 2\pi/n\Delta x$, where n is the number of data points and Δx is the spacing between them. As expected, Δk decreases as the path length increases, i. e. as n or Δx increases. To improve on this somewhat poor value of Δk (which is due to complex Fourier transforms being a fit of n complex parameters to n complex values), we perform a non-linear least squares fit of the data to a sum of traveling plane waves. We fit one plane wave for each mode excited (i. e., each peak in the Fourier transform). To help the program converge to meaningful values, the approximate values of k found in the Fourier transform are used as initial values. An exponential attenuation is included, which sometimes helps to model the changing properties of the liquid bond as the scan progresses. As mentioned earlier, we do not expect the total amplitude of the detected signal to be very reliable. A typical fit to superposed shear and longitudinal modes is shown as the solid line in Fig. 4. Note that the fit reproduces all of the qualitative features of the experimental results, but that the amplitude of some of the peaks is not well matched.

From the fitted values of k and from the density, ρ, we can calculate the flexural (F) or shear ($S_z = c_{66}$, with the z axis normal to the plane of the film) modulus using the equations:

$$\frac{\omega}{k_{SO}} = \sqrt{\frac{F}{\rho}} \qquad (1a)$$

$$\frac{\omega}{k_{SH}} = \sqrt{\frac{S_z}{\rho}} \; . \qquad (1b)$$

Because thin films tend to grow with a preferred texture along the plane normal

and are usually polycrystalline within the plane, they possess uniaxial (hexagonal) or higher symmetry (cubic, isotropic). In the uniaxial case, we have:

$$S_z = c_{66} = \frac{(c_{11} - c_{12})}{2} \tag{2a}$$

$$F = c_{11} - \frac{c_{13}^2}{c_{33}} \tag{2b}$$

$$E = \frac{(c_{11} - c_{12})\,(c_{33}\,(c_{11} + c_{12}) - 2c_{13}^2)}{c_{11}c_{33} - c_{13}^2} = 4S_z\,(1 - S_z/F) \tag{2c}$$

$$B = c_{11} + c_{12} - \frac{2c_{13}^2}{c_{33}} = 2\,(F - S_z) \tag{2d}$$

where the c_{ij}'s are the elements of the elastic stiffness tensor in the two index notation, E is Young's modulus and B is the biaxial modulus.[10] The expressions for E and B as a function of F and S_z do not increase our knowledge of the fundamental constants of the material (i. e., of the c_{ij}'s), but they are convenient and useful macroscopic variables that have direct physical applications.

4 Elastic moduli of textured films of pure metals

We tested the experimental technique using a set of textured films of pure metals. Our measurements of F and S_z, together with the derived values of E and B, are shown in Table 1. For each sample, we usually repeated the experiment until four good traces were obtained: i. e., we required sharp peaks in the Fourier transform, and a least squares fit reproducing well all of the features of the experimentally measured

amplitudes (Fig. 4 and 5 represent satisfactory results).

We observed that the initial measurements were often more reliable than the subsequent ones because the solid bond eventually degraded and broke if too much tension was applied or if the film was mishandled.

The shear waves are not observed in all films. We have found that the "yaw" angle of the receiving IDT can sometimes suppress either the longitudinal or (more commonly) the shear wave. This effect is larger with wider films and for shorter ultrasonic wavelengths since the angle must then be adjusted more carefully. In many instances, however, the shear wave was never seen, even after the experiment was repeated for several different angles. We suspect that the quality of the solid bond plays a role in how much of the shear motion is transmitted to the film. We noticed that as we became more proficient at mounting the film, the shear wave was observed more consistently. It is also possible that the amount of oil (used as the ultrasonic link between the film and the receiving IDT) plays a role in absorbing the shear energy, or in decreasing the effective position resolution below what is needed to observe the shorter wavelengths associated with the shear wave.

When we average four experiments for as same film, we can determine the standard deviation in the measurements of F and S to be roughly ± 3 % and ±1.5 % respectively (The standard deviation on S is half that of F because the shear wavelength is about half that of the Lamb symmetric wavelength). This corresponds to an accuracy of ± 1.5 % and ± 0.8 % in k and in the ultrasonic velocity. The inter-sample errors were larger by about a factor of about two, possibly due to the way the films were mounted, defects or other geometric or structural parameters. Table 2 shows the calculated upper and lower estimates of the expected values of the moduli for these

films. They were calculated by doing elastic stiffness and compliance polycrystalline averages for textured films.[10] These averages represent upper and lower bounds on the c_{ij}'s and s_{ij}'s respectively. From these two sets of constants, we calculated the above minimum and maximum estimates. Within our experimental accuracy, the measured moduli were found to lie between these estimates.

5 Application to Cu-Pd Multilayers

This new method of measuring the phase velocity of ultrasounds in unsupported thin films was developed as an alternative to study the mechanical behavior of artificial metallic superlattices, and in particular, to determine if the controversial supermodulus effect exists.

This effect was observed in the [111] textured Cu-Pd system by Yang[11] and in other [111] textured systems that form solid solutions, such as Au-Ni[11], Ag-Pd[12] and Cu-Ni.[13,14,15] For the Cu-Pd system, Yang observed a sharp stiffening of the biaxial modulus as the modulation amplitude of a thin foil (Λ = 15 Å) increased. The measured value for B was up to four times larger than both the measured value for a film of Λ = 69 Å and the calculated value using the classical analysis presented earlier. The other systems also showed enhancements of their biaxial, flexural, Young's and shear (S_x) moduli by factors of between two and four.

The measurements on the Cu-Pd system were repeated by Itozaki[16] who did not observe any increase in B. Much controversy arose as to the reasons for this discrepancy.[16,17] The Cu-Pd measurements were performed using a bulge tester and a

self-supporting film. The other systems were also studied using self-supporting films and combinations of vibrating reed techniques, stress-strain gauges and a torsion pendulum. All of these direct methods of measurement present many experimental difficulties such as bonds that deform under tension, curvature effects, wrinkles in the micron thick foils, effects of defects and jagged edges.

In contrast, ultrasonic measurements are much less susceptible to the above difficulties. Recent results using Brillouin scattering[18] and the method presented here[19] have not provided any evidence for the supermodulus effect in Cu-Ni. As we will see shortly, our new measurements of the Cu-Pd system also support the case against the effect.

The Cu-Pd multilayers studied here were prepared by electron beam evaporation onto a mica substrate in a vacuum of better than 2×10^{-8} Torr and at a deposition rate of 2 Å/s. A 1500 Å base layer of Cu was first deposited at a substrate temperature of 300 °C to insure good [111] growth. Thereafter, alternate layers of Cu and Pd were deposited at substrate temperatures of 75 to 80 °C. The composition modulation wavelength, Λ, and the first Fourier component of the amplitude of modulation, A_1, were determined with X-rays using the method described by Mattson.[18] The results are shown in Table 3. We also determined the effective lattice spacing to be 2.169 ± 0.003 Å and to be independent of the composition modulation wavelength.

The measured values of the elastic moduli are shown in Fig. 6. We calculated the elastic stiffness tensor of the multilayer using the formalism of Grimsditch and Nizzoli.[20] They assumed that the total stress and strain are equal to the weighted sum (by volume) of the individual stresses and strains in each material. The effect of the

layer structure is to impose particular boundary conditions at the interfaces. These assumptions are valid in the special case where the ultrasonic wavelength is very long compared to the layer thickness, and they do not include any anomalous effect. The base Cu layer's effect on the film is to increase the relative fraction of copper. This formalism allows us to calculate the effective elastic stiffness tensor of a perfect multilayer, and we also derived an equivalent procedure to calculate the effective compliance tensor. Since our films are polycrystalline aggregates, we averaged these two tensors in the plane of the film to obtain upper and lower bounds on the c_{ij}'s and the s_{ij}'s. These averaged constants are then used to calculate upper and lower estimates for the expected moduli of our Cu-Pd films. The estimates are shown as dashed lines in Fig. 6 (for the biaxial modulus, these two estimates coincide).

Our measured moduli for the Cu-Pd superlattices tend to agree with the calculated lower estimates. This is more evident for the shear modulus. On the other hand, the large scattering of the results for the flexural modulus, especially below Λ = 25 Å, could possibly indicate problems in growing multilayers of similar and uniform properties at short wavelengths.

These ultrasonic measurements show that the elastic moduli of the Cu-Pd multilayer system are independent (to our experimental resolution) of the composition modulation wavelength, and do not show any evidence for the supermodulus effect. The larger than expected fluctuations in the measurements of F below Λ = 25 Å seem unrelated to the large increase in B measured by Yang. On the other hand, a possibility remains that impurities or some external and uncontrolled factor can influence the flexural modulus of the Cu-Pd system.

6 Concluding remarks

Although this novel technique was used to observe thin film vibration modes, it could easily be adapted to measure Rayleigh waves. It is also possible to use a laser interferometer to replace the receiving IDT.[9] This offers better position resolution and removes the problems associated with the liquid bond. This method of detection however, requires the sample to be reflective and also increases the complexity and cost of the overall experiment.

Acknowledgement

This work was supported by the Office of Naval Research under the grant ONR N0014-88-K-0160.

Figure Captions

1) Schematic of the IDT's, film and the support arrangement: a) electrodes, b) $LiNbO_3$ substrate, c) film, d) liquid bond, e) varnish, f) mica support, g) string, h) receiving IDT.

2) a) Side and b) top view of the apparatus. In (b), only the sample holder is shown. Translators are represented as a crossed-hashed parts which move with respect to a darker base. Adjustment screws are shown horizontally or vertically hatched. The various parts are: a) receiving IDT enclosure, b) vertical translator, c) optical mount, d) receiving IDT, e) precision translator, f) film holder mounting plate, g) DC motor with optical encoder, h) emitting IDT, i) brass block, j) brass plate, k) translator, l) string, m) film, n) weight.

3) Electronic set-up. The 2 ADC's, the computer and the driver for the precision translator are not shown.

4) Real component of the complex ultrasonic amplitude in a Cu-Pd thin film. The dots are the measured data points and the solid line represents a least squares fit to a sum of traveling waves.

5) Power spectrum as a function of the k vector. The two positive peaks represent the Lamb symmetric ($k = 15.76\ mm^{-1}$) and shear ($k = 31.73\ mm^{-1}$) modes.

6) a) Flexural, b) shear, c) Young's and d) biaxial moduli of Cu-Pd superlattices as functions of layer thickness. The Young's and biaxial moduli are derived from the flexural and shear moduli using the uniaxial symmetry properties of the films. The

dashed horizontal lines represent upper and lower estimates on the expected moduli. All values are given in GPa.

Table 1: Measured moduli of [111] textured films of pure metals.

L (Å)	Thickness (mm)	F (GPa)	S (GPa)	E (GPa)	B (GPa)
[111] Cu	---	178 ± 2	---	---	---
[111] Ag	1.59	111 ± 3	28.2 ± 0.2	84.2	166
[111] Pd	1.38	192 ± 4	47.0 ± 0.4	142	290
[111] Pd	1.38	204 ± 6	47.7 ± 0.8	146	313
[111] Pd	1.31	206 ± 13	45.0 ± 0.7	141	322

Table 2: Calculated upper and lower bounds for the flexural, shear (S_z) and Young's moduli using the bulk elastic constants found in ref. 13. All values are given in GPa.

Film	F_{max}	F_{min}	$S_{z,max}$	$S_{z,min}$	E_{max}	E_{min}	B_{min}	B_{max}
[111] Ag	120.0	111.7	35.1	27.3	099.4	082.5	169.8	168.8
[111] Cu	188.7	174.0	58.2	43.4	160.9	130.3	261.0	261.2
[111] Pd	200.2	188.7	56.3	44.7	161.9	136.5	287.8	287.8
Cu-Pd	193.8	180.5	57.3	44.0	161.4	133.1	273.0	273.0

Table 3: Wavelength (Λ) and amplitude (A_1) of the first Fourier component of the modulation, flexural (F), shear (S_z), Young's (E) and biaxial (B) moduli for composition modulated Cu-Pd thin films. The moduli were evaluated assuming that the density of Cu and Pd are 8.96 g/cm^3 and 12.02 g/cm^3, respectively.

Λ (Å)	Thickness (mm)	A_1	F (GPa)	S (GPa)	E (GPa)	B (GPa)
12.98	1.45	0.17	167	46.1	134	242
14.84	1.43	0.15	153	44.1	126	217
15.03	1.45	0.15	190	---	---	---
16.55	0.98	0.17	171	45.8	134	250
17.69	1.48	0.15	197	48.4	146	297
20.21	1.50	0.15	207	45.0	141	324
21.33	1.43	0.17	175	44.5	133	261
21.62	0.98	0.23	183	44.9	136	276
23.25	1.55	0.19	160	43.9	128	232
25.11	1.52	0.22	175	43.7	131	262
26.18	1.46	0.21	176	---	---	---
28.60	1.47	0.24	180	44.2	133	271
29.43	1.43	0.24	183	---	---	---
32.86	1.48	0.25	171	43.3	129	255
35.51	1.40	0.28	199	---	---	---

[1] I. L. Gelles. J. Acoust. Soc. Am. **40** 1 (1966) p.138.

[2] Kiyohiko Uozumi and Akira Kinbara. Japan. J. Appl. Phys. **10** (1971) p. 950.

[3] K. Uozumi, T. Nakada and A. Kinbara. Thin Solid Films **12** (1972) p. 67.

[4] D. A. Hutchins and K. Lundgren. Rev. Prog. in Quant. Nondest. Eval. **7A** p. 79.

[5] R. J. Dewhurst, C. Edwards , A. D. W. McKie and S. B. Palmer. Appl. Phys. Lett. **51** 14 (1987) p. 1066.

[6] J.-P. Monchalin, J.-D. Aussel, R. Héon, C. K. Jen, A. Boudreault and R, Bernier. Submitted to J. Nondest. Eval., Special Issue on Optical Methods (1989). R. B. Thompson Ed., Plenum, N. Y.

[7] R. Bhadra, M. Grimsditch, Ivan K. Schuller and F. Nizzoli. Phys. Rev. **B39** 17 (1989) p. 12456.

[8] B. A. Auld. *Acoustic Fields and Waves in Solids.* Wiley, New York, c1973.

[9] A. Moreau, J. B. Ketterson and J. Huang. To be published in Mat. Sci. and Eng. A, 1990.

[10] D. Baral, J. E. Hilliard, J. B. Ketterson and K. Miyano. J. Appl. Phys. **53** 5 (May 1982) p. 3552.

[11] W. M. C. Yang, T. Tsakalakos and J. E. Hilliard. J. Appl. Phys. **48** 3 (1977) p. 876.

[12] G. E. Henein and J. E. Hilliard. J. Appl. Phys. **54** 2 (1983) p. 728.

[13] T. Tsakalakos and J. E. Hilliard. J. Appl. Phys. **54** 2 (1983) p. 734.

[14] L. R. Testardi, R. H. Willens, J. T. Krause, D. B. McWhan and S. Nakahara. J. Appl. Phys. **52** 1 (1981) p. 510.

[15] D. Baral, J. B. Ketterson and J. E. Hilliard. J. Appl. Phys. **57** (1985) p. 1076.

[16] H. Itozaki. Ph. D. Thesis, Northwestern University (1982).

[17] D. Baral. Ph. D. Thesis, Northwestern University (1983).

[18] J. Mattson, R. Bhadra, J. B. Ketterson, M. Brodsky and M. Grimsditch. To be published in J. Appl. Phys., 1990.

[19] A. Moreau and J. B. Ketterson. Submitted to Appl. Phys. Lett. 1990.

[20] M. Grimsditch and F. Nizzoli. Phys. Rev. **B33** (1986) p. 5891.

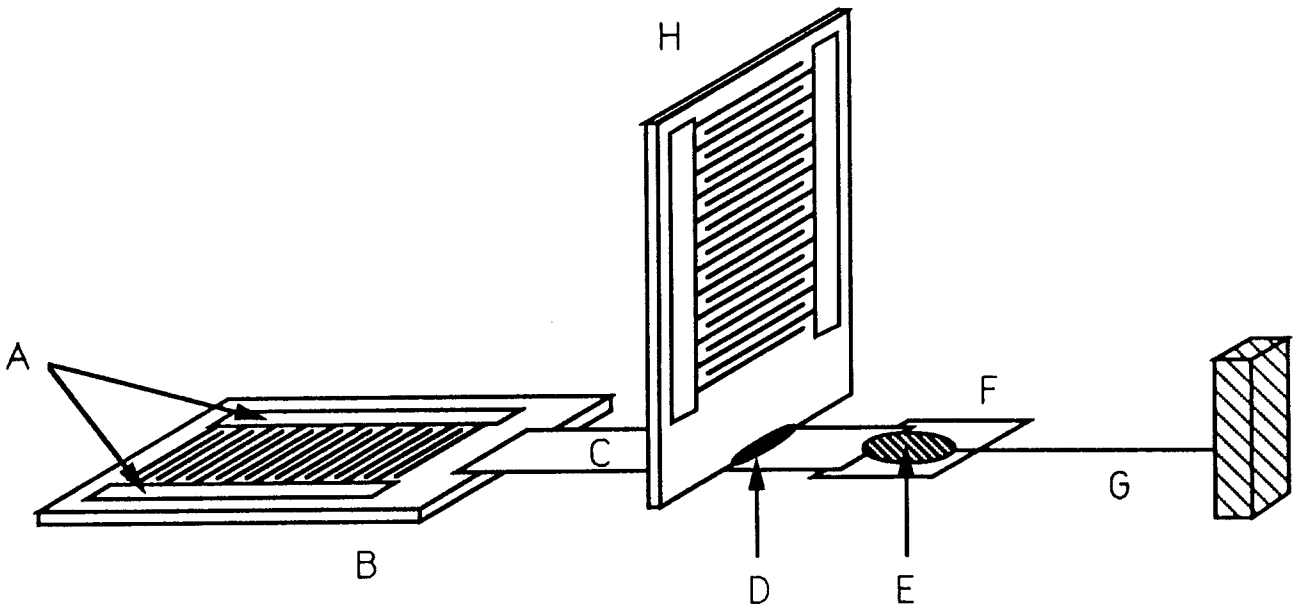
H
A
F
C
G
B
D
E

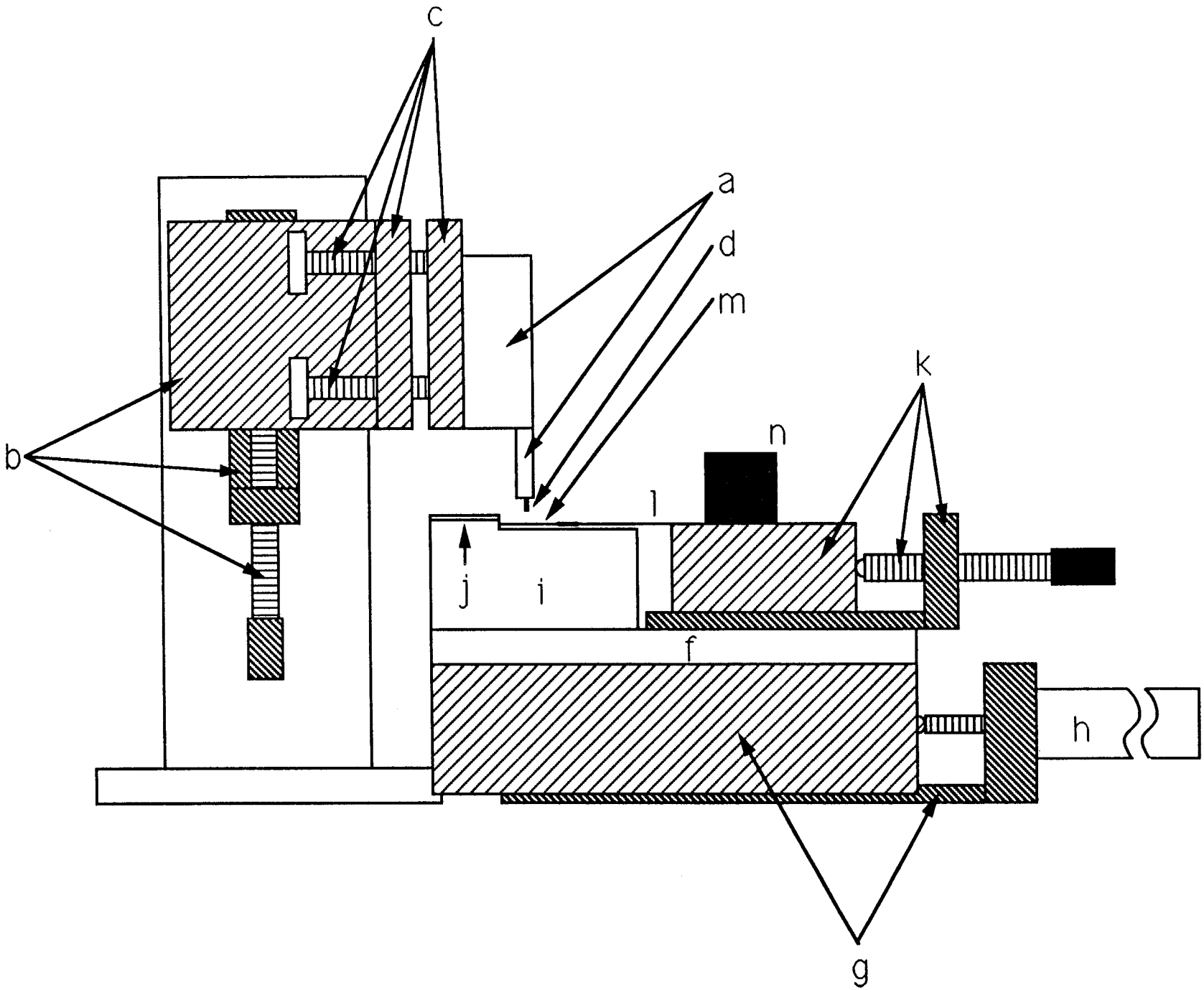
c
a
d
m
k
n
b
l
j
i
f
h
g

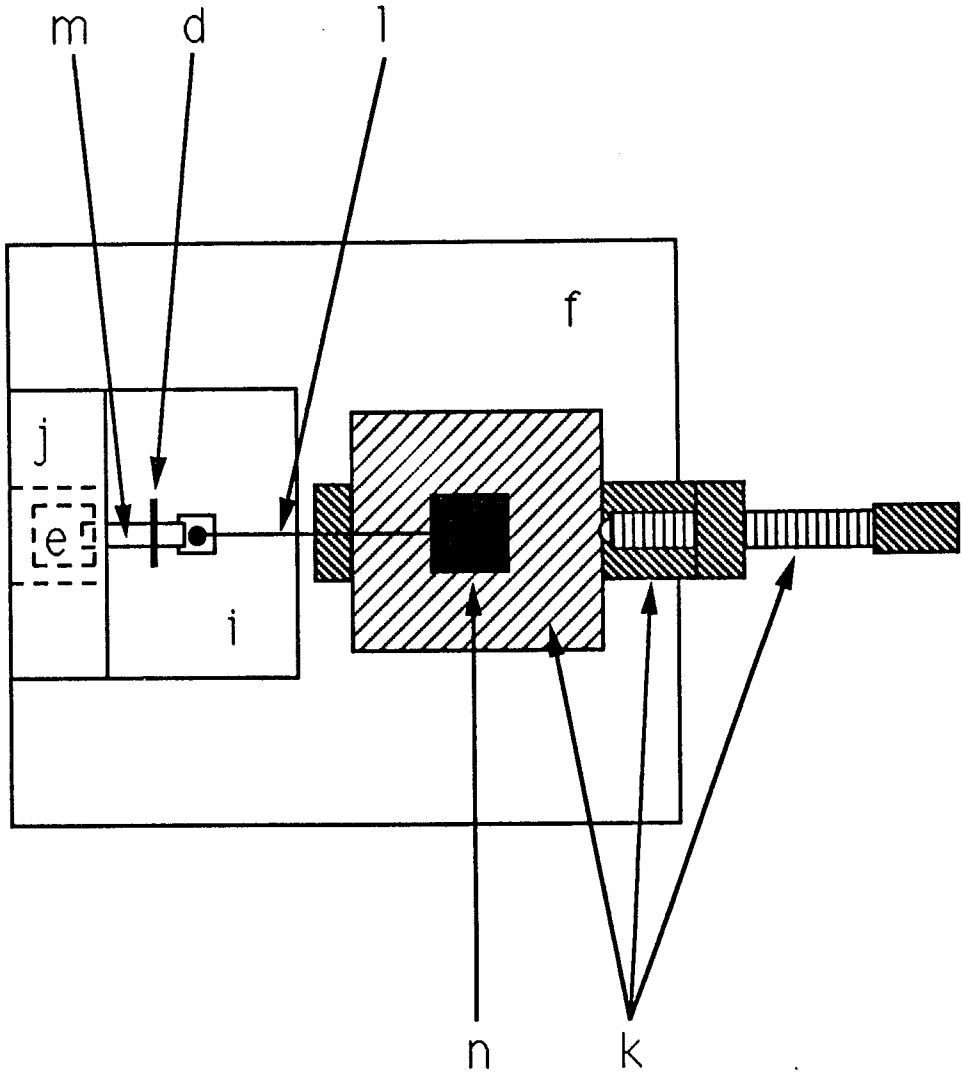
m
d
l
f
j
e
i
n
k

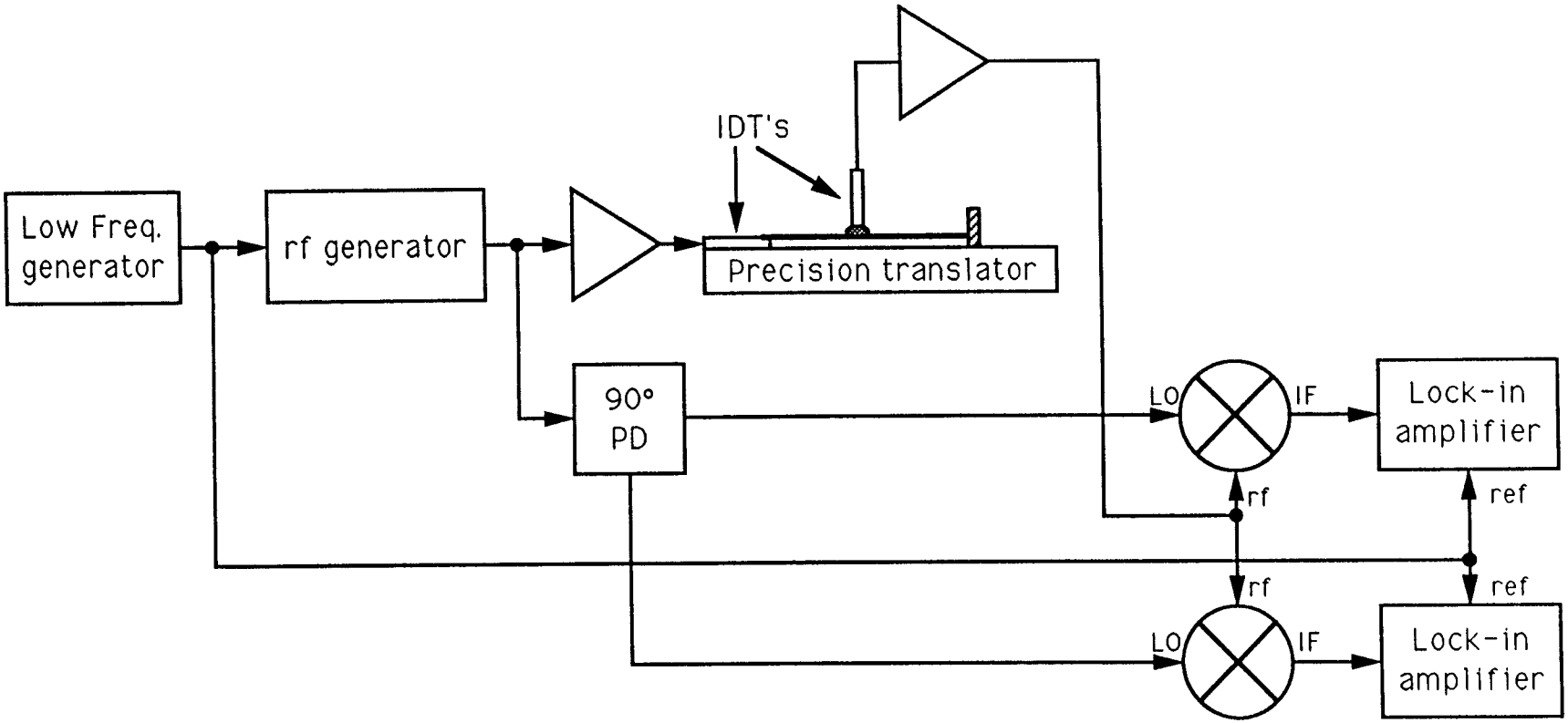
Low Freq. generator
rf generator
IDT's
Precision translator
90° PD
LO
IF
Lock-in amplifier
rf
ref
rf
ref
LO
IF
Lock-in amplifier

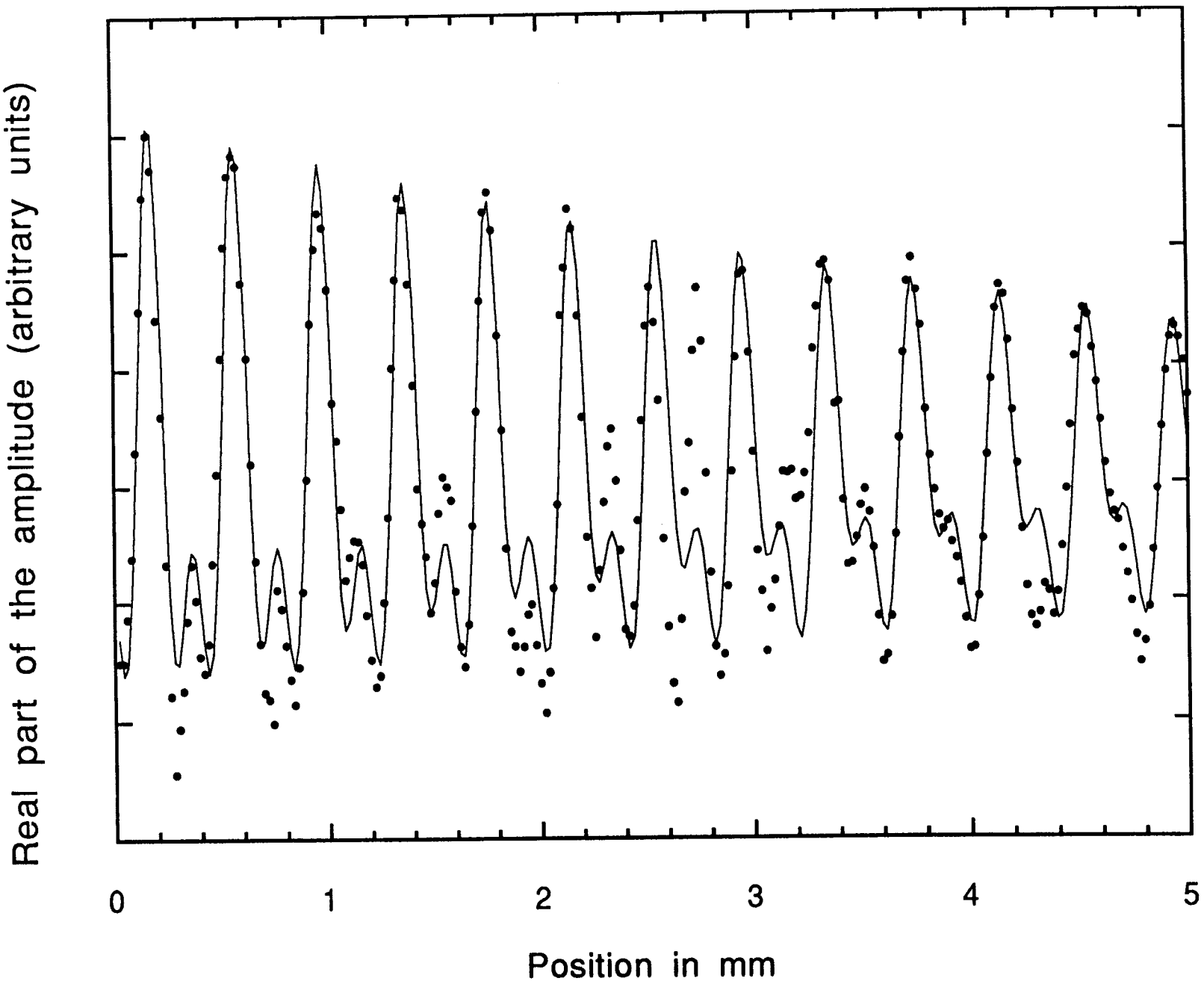
Real part of the amplitude (arbitrary units)
0
1
2
3
4
5
Position in mm

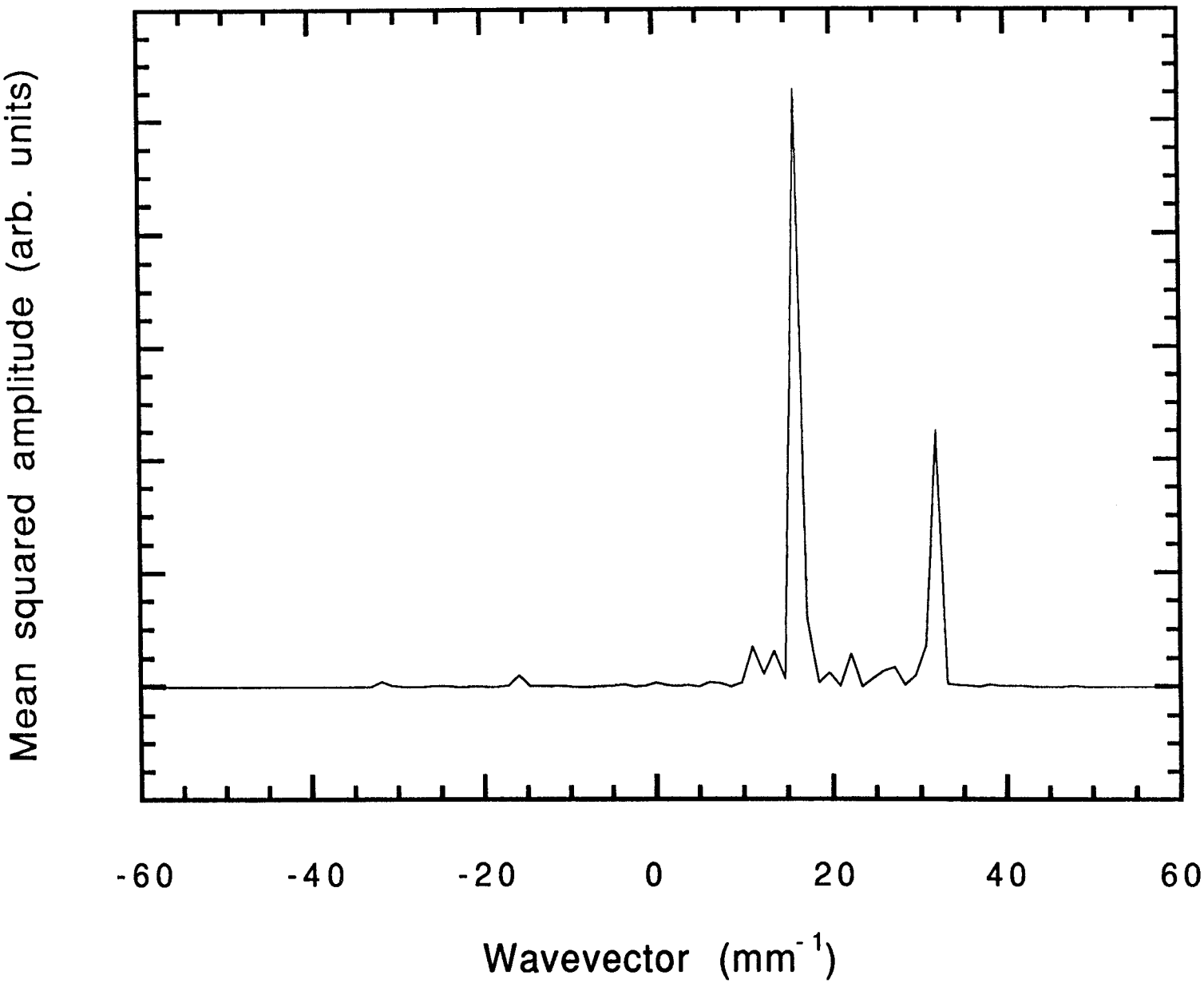
Mean squared amplitude (arb. units)
-60
-40
-20
0
20
40
60
Wavevector (mm^{-1})

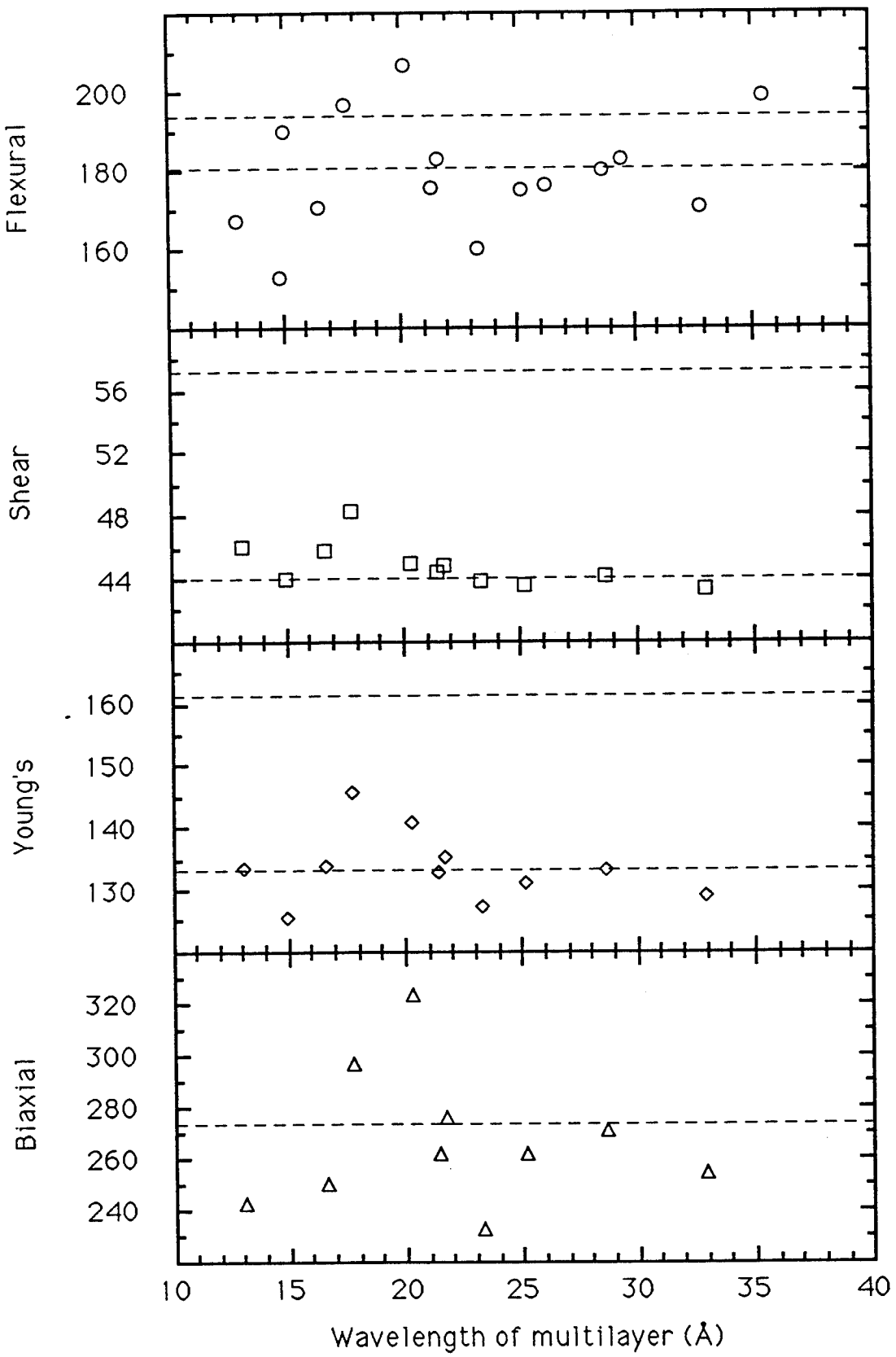
Flexural
200
180
160
Shear
56
52
48
44
Young's
160
150
140
130
Biaxial
320
300
280
260
240
10
15
20
25
30
35
40
Wavelength of multilayer (Å)